Examining HIV Progression Mechanisms via Mathematical Approaches

Wenjing Zhang
Department of Mathematics and Statistics, Texas Tech University

Ramnath Bhagavath, Neal Madras and Jane M Heffernan
Department of Mathematics and Statistics, York University

July 17, 2019

Abstract

The progression of HIV infection to AIDS is unclear and under examined. Many mechanisms have been proposed. That includes a decline in immune response, increase in replication rate, involution of the thymus, syncytium inducing capacity, activation of the latently infected cell pool, chronic activation of the immune system, and the ability of the virus to infect other immune system cells. But their significance is unknown. We develop a simple HIV viral dynamics model incorporating proposed mechanisms as parameters. The conditions for backward and forward bifurcations are derived in the entire parameter space. Detailed relations between model parameters and output behaviors are revealed through a global uncertainty and sensitivity analysis, and further through 1- and 2-parameter bifurcation analysis. Our results indicate that the progression is mainly contributed by changes in characteristics of the productively and latently infected CD4 T-cell pools, the production of free virus from other cells pools, and immune system exhaustion.

Keyworks: HIV progression, numerical bifurcation analysis, global uncertainty, and sensitivity analysis

1 Introduction

HIV can infect all cells in the immune system and the central nervous system which have a CD4 receptor on the cell surface, including T helper cells, monocytes, macrophages, and dendritic cells. However, the main target of the HIV virus is the CD4 T-helper lymphocyte, the main driver of the immune response. A large reduction in the number of CD4 T-helper cells seriously weakens the immune system, affecting the ability

to fight opportunistic diseases. When the CD4 T-cell count reaches a measurement below 200 cells per microlitre of blood, a patient is diagnosed with AIDS. Treatment with antiviral therapy can delay the onset of AIDS, but this depends on drug adherence and the evolution of drug resistance.

The progression of HIV to AIDS is marked by a decrease in the CD4 T-cell count, and an increase in the viral load. The mechanism by which HIV infection transforms into AIDS is unclear (Cloyd et al, 2000). Several factors such as a decline in immune response (Feinberg and McLean, 1997; Dubrow et al, 2012), increase in replication rate (Biesinger and Kimata, 2008; Langford et al, 2007; Selhorst et al, 2017), involution of the thymus (Ye et al, 2004; Beltz, 1999), syncytium inducing capacity (Feinberg and McLean, 1997; Kwa et al, 2001), activation of the latently infected cell pool (Grossman et al, 1998; Dahabieh et al, 2015; Rong and Perelson, 2009; Chun et al, 1998; Ruelas and Greene, 2013; Callaway and Perelson, 2002), chronic activation of the immune system (Paiardini and Müller-Trutwin, 2013; Klatt et al, 2013; Sereti and Altfeld, 2016; Hsu and Sereti, 2014; Hazenberg et al, 2003), and the ability of the virus to infect other immune system cells (Orenstein et al, 1997; Vazeux et al, 1987; Till et al, 1988; Cunningham et al, 2010) have been associated with HIV progression to AIDS. However, it is not known what factors most drive disease progression. Mathematical modeling is well suited to provide insight into this complex process (Anderson and May, 1992; Murray et al, 1989; Nowak and May, 2000).

Mathematical modeling studies of HIV infection in-host are abundant in the literature. The vast majority of these studies, however, focus on the acute and latent stages of infection. Mathematical models of HIV progression to AIDS are presented by Wodarz and Nowak (2002),Alizon and Magnus (2012), Fraser et al (2014), and Culshaw (2006). While these models have been successful in presenting T-cell count and viral load curves which demonstrate HIV progression to AIDS, these studies have fallen short of determining what characteristics of the underlying biology most drive the decline in CD4 T-cells and increase in viral load. This may be due to the fact that many of these studies include models composed of a large number of equations, making model analysis very difficult. The majority of these studies also include a large number of unknown parameters, therefore identifying model parameters linked to specific biological processes which drive HIV progression can be difficult.

We have developed a mathematical model of HIV infection in-host progression to AIDS consisting of three ordinary differential equations. The model includes the effects of thymic involution, density dependent proliferation of CD4 T-cells, and a growth term in the productively infected cell pool signifying the addition of infected cells from other infected cell pools including the latently infected cell pool. The model is presented in Section 2. Most of the analytical results are presented in Section 3. The basic reproduction number R_0 is derived in different approaches and proved equivalent. The conditions for the occurrence of backward and forward bifurcations are derived on the 1-dimensional center manifold when $R_0 = 1$. Sensitivity analysis and bifurcation analysis on the endemic equilibrium are presented in Section 4. Finally, in Section 5 we discuss our results and identify what model parameters most

affect disease progression from HIV to AIDS through numerical bifurcation analysis.

2 Model

The model consists of three ordinary differential equations describing the uninfected and productively infected target cell populations, and the infectious HIV viral load. The model represents a simple extension from the basic model of virus dynamics by Nowak and May (2000), including density dependent proliferation of the T-cells, and time dependent production rates of the target cells. We let x, y, and v respectively represent the number of uninfected T-cells, infected T-cells, and infectious virus particles at time t. The model is as follows:

$$\begin{aligned} \frac{dx}{dt} &= \frac{\lambda}{v+\epsilon} - dx - \beta xv + px\left(1 - \frac{x+y}{T}\right) \\ \frac{dy}{dt} &= \beta xv + ry\left(1 - \frac{x+y}{T}\right) - ay \\ \frac{dv}{dt} &= kqy - uv - \beta xv\,. \end{aligned} \tag{1}$$

All parameters are nonnegative. We assume that they are nonzero unless explicitly stated otherwise. We now describe each equation in more detail:

Equation for x: CD4 T-cells are produced by the thymus. It is assumed that the production of these cells depends on the HIV infection, where thymocyte infection occurring during HIV infection induces involution of the thymus (Ye et al, 2004; Beltz, 1999). Therefore, we will exam the influence of the parameter λ on model behavior to represent that CD4 T-cell production decreases as the viral load increases, in the term $\lambda/(v+\epsilon)$, where ϵ represents a saturating value, and is used to implement biological factors associated with the immune system. For example, HIV induced involution of the thymus will not occur immediately upon infection with the HIV virus (G Meissner et al, 2003). To maintain homeostasis in T-cell count in uninfected hosts, T-cells must proliferate to account for the decreasing thymic production (homeostatic proliferation) (Surh and Sprent, 2000). This is represented using density dependent proliferation where T is the carrying capacity and p the proliferation rate. Immune system exhaustion is also represented in this term, since as the infected population increases, the healthy T-cell population will be negatively affected. Similar to the basic model of virus dynamics, uninfected cells either die (rate d) or become infected by HIV virus (βxv).

Equation for y: Productively infected CD4 T-cells are produced by infection of uninfected T-cells by virus (βxv). We also assume that these cells can proliferate

(Chomont et al, 2009) at a rate of r. The proliferation process is modeled by the logistic term $ry(1-(x+y)/T)$. Infected cells die at a rate of a. Note that this model is similar to a model presented by Rong and Perelson (2009), where the latently infected cell pool was considered.

Equation for v: Infectious virus particles are produced from productively infected CD4 T cells and from other types of productively infected cells including monocytes, macrophages and dendritic cells (Van Lint et al, 2013; Chomarat et al, 2003). The production of infectious free virus is represented as kq where k is the number of infectious virions produced by a productively infected CD4 T-cell, and q gives the ratio of the total infected cell pool including CD4 T-cells, monocytes, macrophages and dendritic cells to the productively infected CD4 T-cell pool. Thus, when $q = 1$ only productively infected T-cells produce virus, but as q increases, the production of virus becomes more dependent on productively infected cells of other cell types (Koppensteiner et al, 2012). This allows us to account for a shift in infection to monocytes, dendritic cells and macrophages when there is a limited pool of CD4 T-cells to infect (Ginhoux and Jung, 2014). Note that we have elected not to explicitly model these cell types so as to make the analysis of the model feasible. Infectious virus is lost due to the infection of an uninfected cell (βxv), or is cleared by the immune system (uv). We note that the loss of virus particles in the infection process is ignored in the vast majority of models of HIV infection in-host. However, it has been found that this term can play a role in the infection dynamics (Klasse, 2015; Heffernan and Wahl, 2006b), T-cell count and viral load (Bocharov and Romanyukha, 1994; Hancioglu et al, 2007; Heffernan and Keeling, 2008). Therefore, this term may be important in studying the progression to AIDS.

In the progression of HIV to AIDS changes in a few, or many, of the model parameters may be involved. For example, a decrease in the production of the CD4 T-cell (λ), which represents an aging thymus, or thymic involution, may contribute. Also, it is possible that a change in the death rate of infected cells (a), in the clearance rate of the virus (u), in the production the infected cells (r), or in the production of infectious virus particles (k) may affect disease progression. A shift from the infection of CD4 T-cells to monocytes, macrophages and dendritic cells will also play a role (q). We therefore assume that all model parameters may change slowly with the progression of the infection. This assumption allows us to study the key underlying mechanisms related to HIV progression to AIDS. We formulate an autonomous differential equations model with parameter values varying in feasible ranges. Below, we provide analytical and numerical methods that aid in determining key parameters related to this progression process.

3 Analytical Results

3.1 Analysis on Model Solutions

3.1.1 Well-posedness of the Solutions of the System (1)

We first remark that Equation (1) is reasonable in the sense that no population size can be negative, and no population grows unbounded. For this well-posed problem, we first prove the positivity and then further show boundedness of the solutions of the model (1).

Lemma 3.1 *(Thieme (2003), Theorem A.4) Let* $\mathbb{R}^n_+ = [0, +\infty)^n$ *be the cone of nonnegative vectors in* $\mathbb{R}^n$ *and* $F : \mathbb{R}^{n+1}_+ \to \mathbb{R}^n$ *be locally Lipschitz,* $F(t, x) = (F_1(t, x), \ldots, F_n(t, x))$ *and* $x = (x_1, \ldots, x_n)$*, and satisfy* $F_j(t, x) \geq 0$ *whenever* $t \geq 0$, $x \in \mathbb{R}^n_+$, $x_j = 0$*. Then, for every initial condition* $x^0 \in \mathbb{R}^n_+$*, there exists a unique solution of* $x' = F(t, x)$, $x(0) = x^0$*, with values in* $\mathbb{R}^n_+$*, which is defined on some interval* $[0, b)$, $b > 0$*. If* $b < \infty$*, then* $\limsup_{t \nearrow b} \sum_{j=1}^n x_j(t) = \infty$.

Theorem 3.1 *Assume that the initial conditions for the system (1) are non-negative. Then the solution of (1) exists and is nonnegative for all* $t \in [0, \infty)$*. Furthermore, the solution is unique and bounded.*

Proof 3.1 We shall apply Lemma 3.1. For $(x, y, v) \in \mathbb{R}^3_+$*, we obtain*

$$\frac{dx}{dt}(0, y, v) = \frac{\lambda}{v + \epsilon} > 0, \quad \frac{dy}{dt}(x, 0, v) = \beta x v \geq 0, \quad \text{and} \quad \frac{dv}{dt}(x, y, 0) = kqy \geq 0.$$

The nonnegativity of the solutions follows. Next, we prove that every nonnegative solution of model (1) *is attracted to the bounded set*

$$\left\{(x, y, v) \in \mathbb{R}^3_+ \,|\, x + y < B + 1,\ v < \frac{kq(B+1)}{u} + 1\right\}, \quad \text{where}$$

$$B = \frac{1}{d^*}\left(\frac{(p+r)T}{4} + \frac{\lambda}{\epsilon}\right) \quad \text{and} \quad d^* = \min\{d, a\},$$

and hence that $b = \infty$*. Using the elementary inequality* $z(1 - z/T) \leq T/4$*, we have*

$$\begin{aligned}\frac{d(x+y)}{dt} &= \frac{\lambda}{v+\epsilon} - dx + px\left(1 - \frac{x+y}{T}\right) + ry\left(1 - \frac{x+y}{T}\right) - ay \\ &\leq -d^*(x+y) + \frac{(p+r)T}{4} + \frac{\lambda}{\epsilon},\end{aligned}$$

from which we obtain $\limsup_{t\to+\infty}(x + y) \leq B$.

As to the virus population, we obtain for large t *that*

$$\frac{dv}{dt} = kqy - uv - \beta x v \leq kqy - uv \leq k\,q\,(B+1) - u\,v,$$

from which it follows that $\limsup_{t\to+\infty} v(t) \leq kq(B+1)/u$*. The proof is finished.*

3.1.2 Steady States

To get the equilibrium solutions of model (1), we set the right sides of the three equations equal to zero as follows:

$$\begin{array}{ll} f_1 & = \dfrac{\lambda}{v+\epsilon} - dx - \beta xv + px\left(1 - \dfrac{x+y}{T}\right) = 0, \\ f_2 & = \beta xv + ry\left(1 - \frac{x+y}{T}\right) - ay = 0, \\ f_3 & = kqy - uv - \beta xv = 0. \end{array} \tag{2}$$

Firstly, the third equation in (2) gives

$$y \;=\; \left(\frac{u+\beta x}{kq}\right) v \tag{3}$$

Then we substitute Eqn (3) for v in the second equation in Eqn (2) and obtain

$$y\left[\beta x\frac{kq}{u+\beta x} + r\left(1 - \frac{x+y}{T}\right) - a\right] \;=\; 0. \tag{4}$$

The first factor from Eqn (4) gives a disease-free equilibrium (DFE), $E_0 = (x_0,\, 0,\, 0)$. Here, x_0 is the non-negative root of

$$\frac{p}{T}\,x^2 \;+\; (d-p)\,x \;-\; \frac{\lambda}{\epsilon} \;=\; 0\,. \tag{5}$$

Since all parameter values are taken positive, there is a unique positive root of Eqn (5), namely

$$x_0 \;=\; \frac{p-d+\sqrt{(p-d)^2+4p\lambda/T\epsilon}}{2p/T}. \tag{6}$$

The second factor from Eqn (4), considering (3), yields v as a function of x, denoted

$$V(x) \;=\; \left(1 \;-\; \frac{a}{r} \;-\; \frac{x}{T} \;+\; \frac{kq\beta x}{r(u+\beta x)}\right) \frac{kqT}{(u+\beta x)}\,. \tag{7}$$

Moreover, assuming that $y > 0$ and $v > 0$, we can rewrite the second equation of (2) as

$$1 \;-\; \frac{x+y}{T} \;=\; \frac{a}{r} \;-\; \frac{\beta xv}{ry} \;=\; \frac{a}{r} \;-\; \frac{\beta kqx}{r(u+\beta x)}.$$

Substituting this into the first equation of (2) shows that any infected equilibrium (x, y, v) must satisfy $\lambda = H(x)$, where we define

$$H(x) \;=\; \left[dx \;+\; \beta xV(x) \;+\; \frac{px}{r}\left(\frac{\beta qkx}{u+\beta x} \;-\; a\right)\right](V(x)+\epsilon)\;. \tag{8}$$

We conclude that the following assertions hold for any given positive parameter values.

(a) Every infected equilibrium is of the form

$$(x, y, v) \;=\; \left(x,\, \left(\frac{u+\beta x}{kq}\right) V(x),\, V(x)\right)\,, \tag{9}$$

and satisfies the equation $\lambda = H(x)$.

(b) Conversely, if $x > 0$, $V(x) > 0$, and $\lambda = H(x)$, then the point given by Equation (9) is an infected equilibrium.

We remark that, given its importance here, λ will be a parameter for further investigation.

3.2 The Basic Reproductive Ratio R_0

The basic reproductive ratio R_0 is defined to be the number of infected cells (or virions) produced by a single infected cell (or virion) when introduced into a totaly susceptible population of target cells (i.e., the DFE $E_0 : (x_0, 0, 0)$). In the present case, two different expressions for R_0 can result, depending on whether infected cells or virions are considered; however, the threshold condition "$R_0 > 1$" for instability of the DFE is valid for both expressions.

3.2.1 Deriving R_0 from a Single Infected Cell Gives R_0^y

First, we consider R_0^y, the number of "next generation" infected cells produced by a single infected cell introduced at the DFE. There are two ways that an infected cell can give rise to new infected cells: (i) by cellular proliferation, and (ii) by producing infectious virions which then infect uninfected cells. For (i), a single infected cell proliferates at rate $r(1-x_0/T)$; since the typical lifetime of an infected cell is $1/a$, we see that a single infected cell produces a total of $r(1-x_0/T)/a$ new infected cells by proliferation. For (ii), a single infected cell produces a total of kq/a infectious virions during its lifetime, and each of these infectious virions has probability $\beta x_0/(u+\beta x_0)$ of infecting a healthy cell before the virion dies. Therefore, we obtain

$$R_0^y \;=\; \frac{r}{a}\left(1-\frac{x_0}{T}\right) \;+\; \frac{kq}{a}\frac{\beta x_0}{u+\beta x_0}\,. \tag{10}$$

$R_0^y > 1$ is the threshold of the emergence of the infected equilibrium E_1. Note that if $r = 0$, then R_0^y is similar to definitions of R_0 found in previous studies which include the viral loss due to infection in the virus equation in Equation (1) Heffernan and Wahl (2006a); Heffernan and Keeling (2008); Heffernan and Wahl (2006b).

3.2.2 Deriving R_0 from a Virion Gives R_0^v

Next we consider R_0^v, the number of "next generation" infectious virions produced by a single infectious virion introduced at the DFE. This is more subtle, because we

need to count possibilities, such as, a virion (called v_1, say) infecting a cell (called c_1), which proliferates to create a new infected cell (c_2), which in turn proliferates to create a new cell (c_3), and this cell c_3 produces a new virion v_2. Although the line from v_1 to v_2 involves several generations of infected cells, it does not involve any other virions; in that sense, we consider virion v_2 to be part of the "next generation" of virions produced by virion v_1. Following this understanding, we define the quantity N^y to be the total number of infected cells descended from a single infected cell by proliferation only (i.e. over all generations but excluding any new infections by virions), including the initial infected cell. If $r = 0$, then $N^y = 1$. If $r > 0$, then N^y satisfies the equation

$$N^y \;=\; 1 \;+\; \frac{r\left(1 - \frac{x_0}{T}\right)}{a}\, N^y \tag{11}$$

because 1 represents the initial cell and $r(1 - x_0/T)/a$ represents the number of first-generation offspring of a single infected cell during its lifetime (as argued for R_0^y above), and each of those first-generation offspring produces a total progeny of N^y over all generations by proliferation alone.

Since the number of infected cells is negligible in this scenario, we only include the uninfected cells x_0 in the density dependence term $r(1 - x_0/T)/a$.

Observe that if $a \leq r\left(1 - \frac{x_0}{T}\right)$, then the only nonnegative solution of Eqn (11) is $N^y = +\infty$. This makes sense because the inequality $a < r\left(1 - \frac{x_0}{T}\right)$ tells us that when y is small, the death rate of an infected cell is less than its proliferation rate, and so the number of infected cells increases. Thus, the population of infected cells will never die out, even if the immune system is 100% effective at immediately killing all free virions; hence N^y is infinite. In contrast, if $a > r\left(1 - \frac{x_0}{T}\right)$, then we can solve Eqn (11) to obtain the finite value

$$N^y \;=\; \frac{a}{a - r\left(1 - \frac{x_0}{T}\right)}\,. \tag{12}$$

Finally, we have

$$R_0^v \;=\; \frac{\beta x_0}{u + \beta x_0}\,\frac{kq}{a}\,N^y \;=\; \frac{\beta x_0}{u + \beta x_0}\,\frac{kq}{a - r\left(1 - \frac{x_0}{T}\right)}, \tag{13}$$

where we should interpret the final expression to be $+\infty$ if it is negative or undefined. Eqn (13) arises because each infectious virion has probability $\beta x_0/(u + \beta x_0)$ of infecting a new cell, which in turn would produce a total of N^y infected cells by proliferation alone, and each of these infected cells would produce kq/a infectious virions. With this interpretation, we easily see that $R_0^v > 1$ if and only if $R_0^y > 1$.

Note again that, if $r = 0$ at the beginning of infection, Eqn (13) is similar to definitions of R_0 found in previous studies which include the viral loss due to infection in the virus equation in Equation (1) in Heffernan and Wahl (2006a); Heffernan and Keeling (2008); Heffernan and Wahl (2006b).

Given the relationship of parameters a and r discussed above, we mark these parameters for further investigation later in this study.

3.2.3 Deriving R_0 from the next generation matrix

Infection process from uninfected (x) to infected (y) cell groups and emission of new viruses (v) from infected cells (y) are considered to be new infections. Then rates of appearance of new infection and rates of transferring between groups are

$$\mathcal{F} = \begin{bmatrix} \beta\, x\, v \\ k\, q\, y \\ 0 \end{bmatrix}, \qquad \mathcal{V} = \begin{bmatrix} -r\, y\, \left(1 - \frac{x+y}{T}\right) + a\, y \\ u\, v + \beta\, x\, v \\ \frac{\lambda}{v+\epsilon} + d\, x + \beta\, x\, v - p\, x\left(1 - \frac{x+y}{T}\right) \end{bmatrix}.$$

Their derivatives evaluated at $E_0 = (x_0,\, 0,\, 0)$ take the partition forms as

$$D\mathcal{F}|_{E_0} = \begin{bmatrix} F & 0 \\ 0 & 0 \end{bmatrix}, D\mathcal{V}|_{E_0} = \begin{bmatrix} V & 0 \\ J_3 & J_4 \end{bmatrix}, \text{ where } F = \begin{bmatrix} 0 & \beta\, x_0 \\ k\, q & 0 \end{bmatrix}, V = \begin{bmatrix} -r\, \left(1 - \frac{x_0}{T}\right) + a & 0 \\ 0 & \beta\, x_0 + u \end{bmatrix},$$
$$J_3 = \begin{bmatrix} \frac{p\, x_0}{T} & \frac{\lambda}{\epsilon^2} + \beta\, x_0 \end{bmatrix}, J_4 = d - p\left(1 - \frac{x_0}{T}\right) + \frac{p\, x_0}{T}.$$

Then the spectral radius of the next generation matrix FV^{-1} is the basic reproduction number

$$R_0 = \rho(FV^{-1}) = \rho\left(\begin{bmatrix} 0 & \frac{\beta\, x_0}{\beta\, x_0 + u} \\ \frac{k\, q\, T}{T\,(a-r) + r\, x_0} & 0 \end{bmatrix}\right) = \sqrt{\frac{\beta x_0}{\beta x_0 + u} \cdot \frac{kq}{a - r + r x_0/T}}. \tag{14}$$

It is easy to see that the basic reproduction number is the square root of the product of the probability of a single infectious virion infecting a new cell and the probability of a single infected cell generating new infectious viruses after infected cell proliferation.

3.3 Linear Analysis for DFE (E_0)

Regarding model (1), the Jacobian matrix associated with its linearized system evaluated at $E_0 = (x_0, 0, 0)$ takes the form:

$$J_0 = \begin{bmatrix} (p-d) - 2\frac{p}{T}\, x_0 & -\frac{p}{T}\, x_0 & (-\beta\, x_0 - \frac{\lambda}{\epsilon^2} \\ 0 & (r-a) - \frac{r}{T}\, x_0 & \beta\, x_0 \\ 0 & k\, q & -\beta\, x_0 - u \end{bmatrix} \tag{15}$$

Its corresponding characteristic polynomial takes the form:

$$P(L) = \det\left[L I_{3\times 3} - J_0\right] = (L + a_{00})\left(L^2 + a_{01} L + a_{02}\right), \text{ where } a_{00} = d - p + \frac{2 p x_0}{T},$$
$$a_{01} = a - r + u + x_0\left(\frac{r}{T} + \beta\right),\ a_{02} = \frac{\beta r x_0^2}{T} + \left[\frac{ru}{T} + (a - r - kq)\beta\right] x_0 + (a-r)u\,. \tag{16}$$

Considering positive values of all parameters and x_0 (that is $x_0 > T(p-d)/(2p)$), we obtain $a_{00} = d - p + 2p\bar{x}_0/T > 0$. we also have $a_{01} > 0$ if $a > r(1 - \frac{x_0}{T})$, assuming that infected cell population dying out is possible. Thus, the first factor of (16) gives a negative real root (or eigenvalue). The roots from the quadratic second factor of (16) take the form $L_{1,2} = \frac{1}{2}\left(-a_{01} \pm \sqrt{a_{01}^2 - 4a_{02}}\right)$. To determine the sign of the real part of L_1 and L_2, we have the following result.

Lemma 3.2 *If $a_{01} \leq 0$, then $a_{02} < 0$. Equivalently, if $a_{02} \geq 0$, then $a_{01} > 0$.*

Proof 3.2 We rewrite a_{02} in (16) *as*

$$\begin{aligned} a_{02} &= (r\,x_0/T + a - r)(\beta\,x_0 + u) - \beta k q x_0 \\ &= [a_{01} - (\beta x_0 + u)]\,(\beta x_0 + u) - \beta k q x_0\,, \end{aligned} \tag{17}$$

from which the lemma is immediate.

Lemma 3.3 *The three roots of the characteristic polynomial $P(L)|_{E_0} = 0$ in Eqn (12) are as follows:*
• *If $a_{02} > 0$: three negative real roots, or one negative real root and a pair of complex conjugate roots with negative real parts;*
• *If $a_{02} = 0$: two negative real roots and one zero root;*
• *If $a_{02} < 0$: one positive and two negative real roots.*
In particular, no root can be purely imaginary.

Proof 3.3 Since the characteristic equation in (16) *has one negative root and the other parameters satisfy Lemma 3.2, the proof is obvious.*

Theorem 3.2 *The DFE, $E_0 = (x_0, 0, 0)$, is a stable node if $a_{02} > 0$, and it is a saddle with 1-dimensional unstable manifold and 2-dimensional stable manifold if $a_{02} < 0$. Moreover, when $a_{02} = 0$, E_0 undergoes a static bifurcation with 1-dimensional center manifold and 2-dimensional stable manifold. Hopf bifurcation does not occur on E_0.*

Proof 3.4 The occurrence of the Hopf bifurcation requires a pair of complex conjugate eigenvalues, which are from the second factor of $P(L)|_{E_0} = 0$ and require the co-occurrence of $a_{01} = 0$ and $a_{02} > 0$. This cannot occur according to Lemma 3.3. The first factor with $a_{00} > 0$ yields a negative root. The other results are derived immediately from Lemma 3.2.

Since the solution of the model (1) is wellposed, it stays positive as $t \to \infty$.

Due to the fact that the DFE is located on the x-axis, no periodic solution encloses the DFE E_0.

Theorem 3.3 *$R_0^y = 1$, $R_0^v = 1$, $R_0 = 1$, and $a_{02} = 0$ are three equivalent thresholds to determine the stability of the DFE.*

Proof 3.5 The condition for stable equilibrium E_0 is

$$a_{02} > 0 \;\Leftrightarrow\; a - r\left(1 - \frac{x_0}{T}\right) \;>\; \frac{\beta x_0}{u + \beta x_0}\, kq \;\Leftrightarrow\; R_0^v < 1 \;\Leftrightarrow\; R_0^y < 1.$$

Similar argument proves that the condition for an unstable equilibrium E_0 is $a_{02} < 0 \;\Leftrightarrow\; R_0^v > 1 \;\Leftrightarrow\; R_0^y > 1$ and the static bifurcation condition is equivalent to the two thresholds, that is $a_{02} = 0 \;\Leftrightarrow\; R_0^v = 1 \;\Leftrightarrow\; R_0^y = 1 \;\Leftrightarrow\; R_0 = 1$.

3.4 Nonlinear Analysis for DFE (E_0)

The Jacobian matrix of the DFE is given as J_0 in (15). Theorem 3.2 indicates that the DFE has a zero eigenvalue when $a_{02} = 0$ (or $R_0 = 1$), which is equivalent to

$$\beta = -\frac{((a-r)T + rx_0)u}{x_0((a-r-kq)T + rx_0)} \triangleq \beta_T \tag{18}$$

The other two eigenvalues, $-a_{00}$ and $-a_{01}$ in (16), are both negative. We choose right and left nullvectors corresponding to the zero eigenvalues as

$$\begin{aligned} v &= \left(\frac{-x_1(T\beta_T kq + \beta_T p x_0 + pu)\epsilon^2 - Tkq\lambda}{((d-p)T + 2px_0)kq\epsilon^2},\, \frac{\beta_T x_0 + u}{kq},\, 1\right)^{tr}, \quad w = (0,\, w_2,\, w_3)\,; \\ w_2 &= (1 + \frac{u}{\beta_T x_0})w_3, \quad w_3 = \frac{\beta_T kq x_0}{\beta_T^2 x_0^2 + 2\beta_T(u + kq/2)x_0 + u^2}. \end{aligned} \tag{19}$$

Moreover, the inner product, $< \cdot, \cdot >$, of column and row vectors (v and u) is one, that is $< w,\, v >= 1$. Let

$$\begin{aligned} B &= w \begin{bmatrix} \frac{\partial^2 f_1}{\partial x \partial \beta} & \frac{\partial^2 f_1}{\partial y \partial \beta} & \frac{\partial^2 f_1}{\partial v \partial \beta} \\ \frac{\partial^2 f_2}{\partial x \partial \beta} & \frac{\partial^2 f_2}{\partial y \partial \beta} & \frac{\partial^2 f_2}{\partial v \partial \beta} \\ \frac{\partial^2 f_3}{\partial x \partial \beta} & \frac{\partial^2 f_3}{\partial y \partial \beta} & \frac{\partial^2 f_3}{\partial v \partial \beta} \end{bmatrix}_{E_0} v = w \begin{bmatrix} 0 & 0 & -x_0 \\ 0 & 0 & x_0 \\ 0 & 0 & -x_0 \end{bmatrix} v \\ &= (1 - \frac{(a-r)T + rx_0}{Tkq})w_2 x_0 = \frac{x_0 kqu}{\beta_T^2 x_0^2 + 2(u + kq/2)\beta_T x_0 + u^2} > 0, \end{aligned} \tag{20}$$

for all positive parameter values and positive disease free equilibrium; and

$$\begin{aligned} A &= \frac{w}{2}(D_{xx}J_0)v^2 = \frac{1}{2} < w,\ (D_{xx}J_0)v^2 >= \frac{1}{2} < w,\ \begin{bmatrix} < v, D_{xx1}v > \\ < v, D_{xx2}\, v > \\ < v, D_{xx3}\, v > \end{bmatrix} >, \\ &= \frac{1}{2}\left((1+\frac{u}{\beta_T x_0}) < v, D_{xx2}v > + < v, D_{xx3}v >\right) w_3, \quad \text{where,} \\ < v, D_{xx2}\, v > &= \frac{1}{((d-p)T+2px_0)T\epsilon^2 kq^2}[-2\beta_T kq^2(\beta_T\epsilon^2 x_0+\lambda)T^2 \\ &\quad +2(\beta_T x_0+u)(-((d-p-kq)r+pkq)\beta_T\epsilon^2 x_0 - ru(d-p)\epsilon^2 + r\lambda kq)T \\ &\quad -2prx_0\epsilon^2(\beta_T x_0+u)^2)], \\ < v, D_{xx3}\, v > &= 2\beta_T \frac{(T\beta_T kq+\beta_T px_0+pu)\epsilon^2 x_0 + Tkq\lambda}{((d-p)T+2px_0)\epsilon^2 kq}. \end{aligned}$$

$$\text{Here,} \quad D_{xxi} = \begin{bmatrix} \frac{\partial^2 f_i}{\partial x\partial x} & \frac{\partial^2 f_i}{\partial x\partial y} & \frac{\partial^2 f_i}{\partial x\partial z} \\ \frac{\partial^2 f_i}{\partial y\partial x} & \frac{\partial^2 f_i}{\partial y\partial y} & \frac{\partial^2 f_i}{\partial y\partial z} \\ \frac{\partial^2 f_i}{\partial z\partial x} & \frac{\partial^2 f_i}{\partial z\partial y} & \frac{\partial^2 f_i}{\partial z\partial z}, \end{bmatrix} \text{ for } i=1,2,3, \quad \text{then}$$

$$D_{xx1} = \begin{bmatrix} -2\frac{p}{T} & -\frac{p}{T} & -\beta_T \\ -\frac{p}{T} & 0 & 0 \\ -\beta_T & 0 & 2\frac{\lambda}{\epsilon^3} \end{bmatrix},\ D_{xx2} = \begin{bmatrix} 0 & -\frac{r}{T} & \beta_T \\ -\frac{r}{T} & -2\frac{r}{T} & 0 \\ \beta_T & 0 & 0 \end{bmatrix},\ D_{xx3} = \begin{bmatrix} 0 & 0 & -\beta_T \\ 0 & 0 & 0 \\ -\beta_T & 0 & 0 \end{bmatrix}. \tag{21}$$

Therefore, A and B in (20) and (21) are coefficients of the center manifold of model (1) at the DFE E_0 when $R_0 = 1$. The center manifold upto third order is written as

$$\dot{u} = A\,u^2 \,+\, B\,u\,\mu \,+\, O(3),$$

Applying the results from Van den Driessche and Watmough (2002) and Castillo-Chavez and Song (2004), we have

Theorem 3.4 *when $R_0 = 1$ or $\beta = \beta_T$, model (1) at the DFE E_0 exhibits a backward (forward) bifurcation if $A > 0$ ($A < 0$).*

4 Uncertainty and Sensitivity Analysis

In the previous analysis we identified three parameters that were critical to determining the existence of the infected equilibrium and the stability of the disease-free equilibrium, namely, λ, r, and a. In the following we determine how changes in these parameters affect the infected equilibrium.

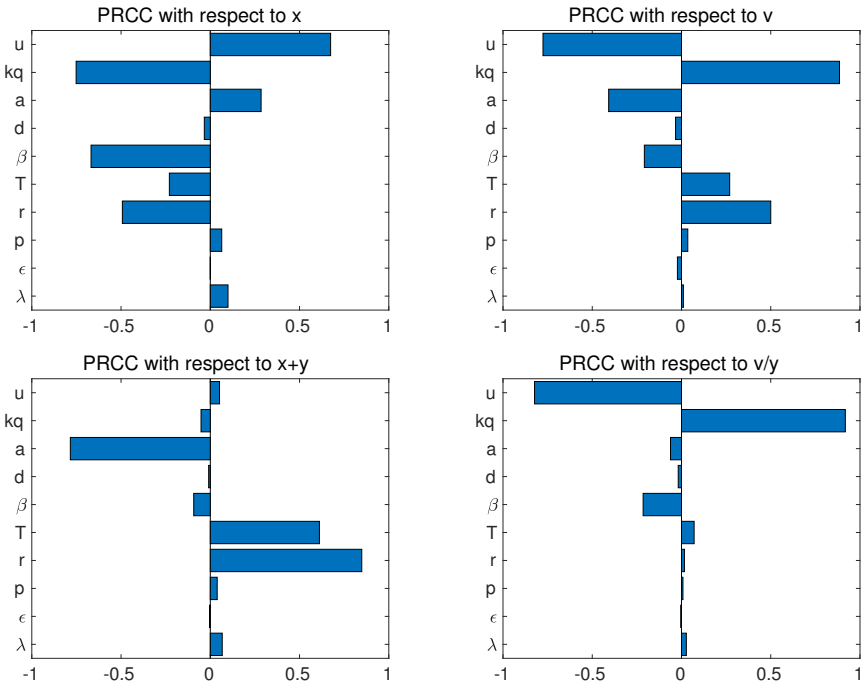

Figure 1: Partial Rank Correlation Coefficients. Parameters: r, a, u, T, β and kq significantly affect the disease progression.

Suppose that we want to say how a stable infected equilibrium changes as one parameter varies, with all other parameters being held constant. For example, Theorem 4.1(i) below says that the x-coordinate of the fixed point is an increasing function of λ. Before we state the results formally, we shall show that the Implicit Function Theorem guarantees that slightly varying a single parameter leads to a differentiable curve of stable fixed points passing through a given stable infected equilibrium.

Suppose (x_0, y_0, v_0) is a stable infected equilibrium corresponding to a particular choice of strictly positive parameter values $(\lambda_0, \epsilon_0, d_0, \beta_0, \ldots)$. (Observe that x_0, y_0, and v_0 are necessarily strictly positive.) We shall focus on λ for concreteness, but the same argument works for any parameter. Define the function $G : (0,\infty)^4 \to \mathbf{R}^3$ by

$$G(x,y,v,\lambda) \;=\; \begin{pmatrix} \frac{\lambda}{v+\epsilon_0} \;-\; d_0 x \;-\; \beta_0 x v \;+\; p_0 x\left(1 \;-\; \frac{x+y}{T_0}\right) \\ \beta_0 x v \;+\; r_0 y\left(1 \;-\; \frac{x+y}{T_0}\right) \;-\; a_0 y \\ k_0 q_0 y \;-\; u_0 v \;-\; \beta_0 x v \end{pmatrix}. \tag{22}$$

Then the fixed point equations used to determine the solutions to (2) are equivalent to writing $G = 0$. Write the 3×4 derivative matrix DG in the block form

$$DG(x,y,v,\lambda) \;=\; (J|w)$$

where J is the 3×3 Jacobian matrix (15) (except that now we treat λ as a variable)

and w is the column vector

$$w \;=\; \begin{pmatrix} \frac{\partial G_1}{\partial \lambda} \\ \frac{\partial G_2}{\partial \lambda} \\ \frac{\partial G_3}{\partial \lambda} \end{pmatrix} \;=\; \begin{pmatrix} \frac{1}{v+\epsilon_0} \\ 0 \\ 0 \end{pmatrix} . \tag{23}$$

By our definition of stability, $\det(J) < 0$ at this equilibrium. Thus the Implicit Function Theorem guarantees the existence of a $\delta > 0$ and a continuously differentiable function $\Phi : (\lambda_0 - \delta, \lambda_0 + \delta) \to (0, \infty)^3$ such that $\Phi(\lambda_0) = (x_0, y_0, v_0)$ and the equation $G(\Phi(\lambda), \lambda) = 0$ holds for every $\lambda \in (\lambda_0 - \delta, \lambda_0 + \delta)$, where we write $\Phi(\lambda) = (x(\lambda), y(\lambda), v(\lambda))$; that is, $\Phi(\lambda)$ is a curve of fixed points parametrized by λ. Since the eigenvalues are continuous functions of the coefficients of the characteristic polynomial (e.g. see Theorem 1.4 of Marden (1989)), we can choose δ small enough so that the fixed point $\Phi(\lambda)$ is stable for every λ in $(\lambda_0 - \delta, \lambda_0 + \delta)$. In particular, the derivatives in the following theorem all exist, and we can safely interpret $\frac{dx}{d\lambda}(\lambda_0)$, for example, to be the rate of change of x with respect to λ at the fixed point (x_0, y_0, v_0).

Theorem 4.1 *At every stable infected equilibrium (x, y, v) with strictly positive parameter values, we have*
(i) $dx/d\lambda > 0$,
(ii) $d(x+y)/d\lambda > 0$,
(iii) $d(v/y)/d\lambda < 0$,
(iv) $dx/da > 0$,
(v) $dv/da < 0$,
(vi) $d(v/y)/da < 0$,
(vii) $sgn(dx/dr) = sgn(x + y - T)$,
(viii) $sgn(dv/dr) = -sgn(x + y - T)$, *and*
(ix) $sgn(d(v/y)/dr) = -sgn(x + y - T)$.

Proof: We first consider varying λ. Differentiating the equation $G(\Phi(\lambda), \lambda) = 0$ with respect to λ gives $J(d\Phi/d\lambda) + w = 0$ (where we write $d\Phi/d\lambda$ as a 3×1 column matrix), or equivalently

$$\frac{d\Phi}{d\lambda} \;=\; -\,J^{-1}w\,. \tag{24}$$

Let K_{ij} be the ij entry of J^{-1}. Then Equations (23–24) show that (omitting the 0 subscripts on the parameters)

$$\frac{dx}{d\lambda} \;=\; -\,\frac{K_{11}}{v+\epsilon}\,, \qquad \frac{dy}{d\lambda} \;=\; -\,\frac{K_{21}}{v+\epsilon}\,, \qquad \frac{dv}{d\lambda} \;=\; -\,\frac{K_{31}}{v+\epsilon}\,. \tag{25}$$

Writing J_{ij} as the ij entry of J, matrix algebra says that

$$K_{11} = \frac{J_{22}J_{33} - J_{23}J_{32}}{\det(J)}\,, \quad K_{21} = \frac{J_{23}J_{31} - J_{21}J_{33}}{\det(J)}\,, \quad K_{31} = \frac{J_{21}J_{32} - J_{31}J_{22}}{\det(J)}\,. \tag{26}$$

At an equilibrium point, the diagonal elements of J given in Eqn (15) can be rewritten as follows. Using the first equation of Eqn (2), we obtain

$$\begin{aligned} J_{11} &= \frac{1}{x}\left(-dx - \beta xv + px\left(1 - \frac{x+y}{T}\right)\right) - \frac{px}{T} \\ &= -\frac{\lambda}{x(v+\epsilon)} - \frac{px}{T} \qquad \text{if } x > 0. \end{aligned} \tag{27}$$

From the second equation of Eqn (2), we obtain

$$\begin{aligned} J_{22} &= \frac{1}{y}\left(ry\left(1 - \frac{x+y}{T}\right) - ay\right) - \frac{ry}{T} \\ &= -\frac{\beta xv}{y} - \frac{ry}{T} \qquad \text{if } y > 0. \end{aligned} \tag{28}$$

And using the last equation of Eqn (2), we obtain

$$J_{33} = -\beta x - u = -\frac{kqy}{v} \qquad \text{if } v > 0. \tag{29}$$

By Equations (25) and (26), together with (28), (29), and Eqn (15),

$$\frac{dx}{d\lambda} = -\frac{\left(-\frac{\beta xv}{y} - \frac{ry}{T}\right)\left(-\frac{kqy}{v}\right) - \beta xkq}{(v+\epsilon)\det(J)} = -\frac{ry^2kq}{Tv(v+\epsilon)\det(J)}, \tag{30}$$

assuming that x, y, and v are all nonzero. In addition, if (x, y, v) is a stable equilibrium, then $\det(J) < 0$, and we see that $dx/d\lambda > 0$. This proves (i).

By Equations (25), (26), and Eqn (15),

$$\begin{aligned} \frac{dy}{d\lambda} &= -\frac{\left(\beta x(-\beta v) - \left(\beta v - \frac{ry}{T}\right)(-u - \beta x)\right)}{(v+\epsilon)\det(J)} \\ &= \frac{\beta^2 xv - \beta vu - \beta^2 xv + \frac{ry}{T}(u + \beta x)}{(v+\epsilon)\det(J)} \\ &= \frac{-\beta vu + \frac{ry^2kq}{Tv}}{(v+\epsilon)\det(J)} \qquad \text{(by (29))}. \end{aligned} \tag{31}$$

Adding Equations (31) and (30) gives

$$\frac{d(x+y)}{d\lambda} = \frac{-\beta vu}{(v+\epsilon)\det(J)}$$

which is positive whenever (x, y, v) is a stable infected equilibrium. This proves (ii).

The proofs for varying a and r are very similar to the arguments for λ, with the following differences. The vector w is now

$$\begin{pmatrix} \frac{\partial G_1}{\partial a} \\ \frac{\partial G_2}{\partial a} \\ \frac{\partial G_3}{\partial a} \end{pmatrix} = \begin{pmatrix} 0 \\ -y \\ 0 \end{pmatrix} \quad \text{or} \quad \begin{pmatrix} \frac{\partial G_1}{\partial r} \\ \frac{\partial G_2}{\partial r} \\ \frac{\partial G_3}{\partial r} \end{pmatrix} = \begin{pmatrix} 0 \\ y\left(1 - \frac{x+y}{T}\right) \\ 0 \end{pmatrix}.$$

The resulting analogues of Equation (25) are

$$\frac{dx}{da} = K_{12}\, y\,, \quad \frac{dv}{da} = K_{32}\, y\,, \quad \frac{dx}{dr} = -K_{12}\, y\left(1 - \frac{x+y}{T}\right), \quad \frac{dv}{dr} = -K_{32}\, y\left(1 - \frac{x+y}{T}\right).$$

We then have from Eqn (15) that

$$K_{12} = \frac{J_{13}J_{32} - J_{12}J_{33}}{\det(J)} = \frac{-(\beta x + \lambda/(v+\epsilon)^2)kq - \frac{px}{T}(u+\beta x)}{\det(J)},$$

which has negative numerator and denominator, and, with the help of Equation (27),

$$K_{32} = \frac{J_{12}J_{31} - J_{11}J_{32}}{\det(J)} = \frac{\frac{px}{T}\beta x v + \left(\frac{\lambda}{(v+\epsilon)x} + \frac{px}{T}\right)kq}{\det(J)},$$

which has positive numerator and negative denominator. These suffice to explain parts (iv), (v), (vii), and (vii).

Finally, parts (iii), (vi), and (ix) follow from the relation $v/y = kq/(u+\beta x)$ (from the fixed point equations of (2)) and parts (i), (iv), and (vii). □

The progression of HIV to AIDS is marked by a decrease in the CD4 T-cell count and an increase in the viral load. The results of Theorem 4.1 show that decreases in CD4 T-cell count are feasible when λ is reduced, a is increased, and if r is increased (but only if $sgn(x+y+T) < 0$). These results also show that the viral load increases when a is decreased and r is increased (but only if $sgn(x+y+T) < 0$).

We now further explore the change in the infected equilibrium with respect to all parameter values, using uncertainty and sensitivity analysis. We conduct uncertainty and sensitivity analysis using Latin Hypercube Sampling (LHS) in McKay et al (1979) and Partial Rank Correlation Coefficients (PRCC) in Anderson (1958). LHS gives adequate quality assurance on model predictions, and PRCC determines the main parameters driving infection.

We perform LHS, using the numerical algorithm described in Marino et al (2008). To perform the LHS method, in the absence of the prior data, we adopt uniform distributions for model parameters using informed parameter value ranges from the modelling and clinical literature (see Table 3). Values were chosen randomly without replacement, and parameter sets that satisfied four filter conditions that ensure that the model equilibria lie within realistic HIV/AIDS ranges were recorded (see Table 1). Following this procedure a PRCC value was calculated for each model parameter. PRCC values range between -1 and 1 with the sign determining whether an increase in the parameter value will decrease (-) or increase (+) the specified model output. A PRCC value $|PRCC| > 0.5$ was considered statistically significant based on empirical knowledge. We chose $100,000$ parameter sets and 910 of these satisfied the filter criteria (Table 1). Finally, within the 910 parameter sets 6 parameter sets produced oscillating simulated solutions for Equation (1), indicating the existence of

a Hopf bifurcation in realistic parameter space. The occurrence of periodic solutions agree with the result from Zhang et al (2016) that backward bifurcation implies rich dynamical behaviors.

The PRCC values relating the model parameters to the infected equilibrium are shown in Figure 1. It shows that parameters: r, a, u, T , β and $k\,q$ significantly affect disease progression. This result confirms the parameters which influence the basic reproduction number R_0. This figure also demonstrates that changes in λ (the production rate of CD4 T-cells) are not significant, whereas, changes in r (the proliferation rate and addition of infected monocytes, macrophages, dendritic cells and activation of latently infected cells) and a (the efficacy of the immune system in killing infected cells) are. It is also shown that changes in other model parameters can have significant effects on the infected equilibrium. In total, the results of the sensitivity analysis show that a reduction in the total CD4 T-cell count $x + y$ can occur as the infected cell death rate a increases and proliferation and/or addition to the infected cell pool r increases. It also shows that an increase in the viral load v can occur when the viral clearance rate u decreases, the viral production rate kq increases, the infected cell death rate a decreases, and proliferation and/or addition to the infected cell pool r increases. Comparing these results, we find that the CD4 T-cell count $x + y$ will decrease and the viral load v will increase when the viral clearance rate u decreases, and the viral production rate kq increases. Interestingly, however, a decrease in the healthy CD4 T-cell count x and an increase in the viral load v can occur when the viral clearance rate u decreases, viral production kq increases, infected cell death rate a decreases (although this is not in the significant range of the sensitivity analysis), and proliferation and/or addition to the infected cell pool r increases. The influence of the infection rate β has direct implications on HIV drug therapy, where the goal is to decrease viral load and increase the healthy CD4 T-cell count. Here, we see that a reduction in β can increase x, however, we cannot conclude any additional effects.

On the other hand, according (12) and (13), the relation between a and r is important to determine the fate of the disease. Figure 1 shows that if the death rate of infected cells (a) decreases, the uninfected CD4 T-cell count (x) will decrease, the infectious viral load (v) will increase, and the ratio of infectious viral load to infected cells (v/y) will increase. Finally, the PRCC results shows that as the proliferation rate of infected target cells, activation of the latently infected cell pool, or infected dendritic cells, monocytes and macrophages pools grow (these are all represented by an increase in r), then the correlation between this parameter r and the uninfected T-cell count (x), infectious free virus (v), and ratio of infectious free virus to infected cell count (v/y) are all determined by the sign of the difference between the total number of uninfected and infected T-cells ($x+y$) and the carrying capacity (T). The magnitude of the correlation, however, was difficult to ascertain in the analysis.

To further compare the influence of any two out of the six parameters: r, a, u, T , β and $k\,q$ on the model behaviors and disease progression, bifurcation analyses are carried out in the next subsection.

5 Bifurcation Analysis on Infected Equilibrium E_1

In this section, we will further investigate how the parameters r, kq, u, β and a affect the disease progression through a bifurcation analysis of (1). Static bifurcation, including saddle-node and transcritical bifurcations, and Hopf bifurcation are computed through symbolic computation. We first evaluate the Jacobian matrix of (1) at E_1, which yields the corresponding characteristic polynomial:

$$\begin{aligned}
P(L\,;\,x,\,y,\,v) &= \det(LI - J|_{E_1}) = L^3 + a_1L^2 + a_2L + a_3, \quad \text{where,}\\
a_1 &= d + a + u - (p+r)(1 - \frac{x+y}{T}) + \frac{1}{T}(px + ry) + \beta(v + x),\\
a_2 &= -(\beta x + u)(C_{11} + C_{22}) - C_{11}C_{22} - \beta v\left[\beta x + \frac{\lambda}{(v+\epsilon)^2}\right] + p\frac{x}{T}(\beta v - \frac{ry}{T}),\\
a_3 &= \left[C_{11}C_{22} + (\beta v - \frac{ry}{T})p\frac{x}{T}\right](\beta x + u) + (kqC_{11} - \beta v p\frac{x}{T})\beta x,\\
&\quad + \left[(\beta v - \frac{ry}{T})kq + \beta v J_{22}\right]\left[\frac{\lambda}{(v+\epsilon)^2} + \beta x\right],\\
C_{11} &= -d - \beta v + p(1 - \frac{x+y}{T}) - p\frac{x}{T},\\
C_{22} &= r(1 - \frac{x+y}{T}) - r\frac{y}{T} - a,
\end{aligned} \tag{32}$$

where y and v take the form of (3) and (7) as

$$y = \frac{(-\beta r x^2 - (T(a - r - kq)\beta + ru)x - Tu(a - r)}{r(\beta x + u)}, \quad v = \frac{kqy}{\beta x + u}, \tag{33}$$

and x is the positive roots of Eqn (34) as follows.

$$\begin{aligned}
F(x) &= c_{10}x^5 + c_{11}x^4 + c_{12}x^3 + c_{13}x^2 + c_{14}x + c_{15} = 0, \quad \text{where,}\\
c_{10} &= \beta^3 r(kq - \beta\epsilon)\left[kq(r-p) + ap - dr\right],\\
c_{11} &= \beta^2(T\beta q^3(p - 2r)k^3 + (2(Ta\beta + ru)q^2(r-p) + T\beta q^2 r[(d+p) + \beta\epsilon] - 2T\beta q^2 r^2)\,k^2\\
&\quad + [T\beta\,(\beta\epsilon r(r-a) + pa^2 + r[rd - a(d+p)]) + 3ru(\beta\epsilon(p-r) + ap - dr)]qk,\\
&\quad + 4\beta\epsilon ru(dr - ap) - \beta^2\lambda r^2),\\
c_{12} &= \beta(T^2\beta^2 q^4 k^4 + (2T\beta(r-a) + u(p-2r))T\beta q^3 k^3,\\
&\quad + (T^2\beta^2 q^2(r^2 + a^2) + 2T\beta q^2(r[\beta(\epsilon u - Ta) + u(d+p)] + 2u[a(r-p) - r^2]) + q^2 r u^2(r-p))k^2,\\
&\quad + 3[T\beta u(r-a)(\beta\epsilon r + dr - ap) + \beta\epsilon r u^2(p-r) + ru^2(ap - dr)]qk,\\
&\quad + 6\beta\epsilon ru^2(rd - ap) - 4\beta^2\lambda r^2 u),\\
c_{13} &= u(2T^2\beta^2 q^3(r-a)k^3 + (2T\beta(r-a)^2 + ru(\beta\epsilon + d + p) + 2u[a(r-p) - r^2])q^2\beta T k^2,\\
&\quad + (3T\beta qu[a^2 p + dr^2 + \beta\epsilon r(r-a) - ar(d+p)] + qru^2[ap - dr + \beta\epsilon(p-r)])k,\\
&\quad + 4\beta\epsilon ru^2(dr - ap) - 6\beta^2\lambda r^2 u),\\
c_{14} &= u^2(T^2\beta k^2 q^2(r-a)^2 + Ta^2 kpqu + Tkqru[\beta\epsilon(r-a) + dr - a(d+p)],\\
&\quad + \epsilon ru^2(dr - ap) - 4\beta\lambda r^2 u),\\
c_{15} &= -\lambda r^2 u^4.
\end{aligned} \tag{34}$$

Theorem 5.1 *The endemic equilibrium $E_1 = (x, y, v)$ undergoes*

1. *a static bifurcation, if $a_3|_{E_1} = 0$, $a_1|_{E_1} > 0$ and and $\Delta_2 > 0$;*
2. *a Bogdanov-Takens bifurcation, if $a_3|_{E_1} = a_2|_{E_1} = 0$ and $a_1|_{E_1} > 0$;*
3. *a Hopf bifurcation, if $\Delta_2 = 0$, $a_1|_{E_1} > 0$ and $a_3|_{E_1} > 0$;*

where a_i, $i = 1, 2, 3$ is coefficient of the characteristic polynomial (32), and $\Delta_2 = a_1 a_2 - a_3$ is the second Hurwitz argument.

We choose two parameters out of r, a, u, T, β and kq and show their influence on the model behaviors through 2-dimensional bifurcation diagrams in Figures 2, 4, and 5. Other parameter values are taken from Tables 2 and 3 in Appendix.

5.1 r vs a

We plot bifurcation diagrams to illustrate the influence of parameter values on behaviors of model (1). We first choose a as the control parameter and r as the bifurcation parameter. Model (1) shows forward bifurcation when $a = 2.9333$ and backward bifurcations when $a = 2.9438$, $a = 3.11$, $a = 3.5$, and $a = 3.8$. Connecting Limit Point (LP) bifurcation points, we have a green limit point curve in Fig. 2 (a) and (b). Connecting the neutral saddle (H) and Hopf bifurcation (H) points, we have a Hopf curve satisfying $\Delta_2 = 0$. Further the Hopf curve denotes Hopf bifurcations plotted in red if $a_3|_{E_1} > 0$, and neutral saddle plotted in magenta if $a_3|_{E_1} < 0$. The sign of $a_3|_{E_1}$ on the Hopf curve changes at Bogdanov-Takens bifurcation (BT). Hopf bifurcation serves as an oscillation source, which induce the oscillating viral load for our model. The stability of the bifurcating limit cycles are determined by the sign of the first Lyapunov coefficient of the corresponding Hopf bifurcation. A positive first Lyapunov coefficient indicates a subcritical Hopf bifurcation, which induces unstable limit cycles; while a negative first Lyapunov coefficient implies a supercritical Hopf bifurcation, which bifurcates stable limit cycles. The zero first Lyapunov coefficient represent an occurrence of a generalized Hopf bifurcation (GH), which is the threshold between subcritical and supercritical Hopf bifurcations. For the parameter values of a and r, indicating the death and proliferation rates of the infected T cells, we plot a close up 2-dimensional bifurcation diagram r vs a in a physically meaningful ranges in Fig. 2 (b). Due to the stiffness of the system (1), numerical bifurcation package is unable to show nice bifurcation curves. Therefore, the closeup in Fig. 2 (b) is plotted according to symbolic computation results, which are consistent with results through Matcont. The blue curve represents branching point (BP) or transcription bifurcation, which is plotted according to $R_0(a, r) = 1$. Here R_0 is the basic reproduction number. Its analytical formula is given in (14). The red Hopf curves are plotted according to the sufficient and necessary conditions in Theorem 5.1. The top Hopf curve represents Hopf bifurcation because the vertical axis range is below the BT point in Fig. 2 (a), that is $a < 3.114226$. Therefore, for positive a and r values,

two parts of red Hopf curves and a blue transcritical curve enclose a parameter range plotted in yellow, in which model (1) demonstrates oscillating viral loads.

Three parameter values of a, $a = 2.9333$, $a = 2.9428$ and $a = 3.8$, are picked up in the yellow region in the closeup of Fig, 2 (b). The corresponding 1-dimensional bifurcation diagrams are plotted in the left column of Fig. 3. Oscillations happen between two supercritical Hopf bifurcations in Fig. 3 (a) and (b). The oscillation peak values x are shown as well. The corresponding oscillation periods are followed on the right panel. Large period viral load oscillation occurs around $r = 0.8$ for both $a = 2.9333$ and $a = 2.9428$. For the case $a = 3.8$, the transcritical bifurcation (BP) occurs at a very large r value. This means the DFE is locally stable in the biologically meaningful region of r. Numerical simulation shows in Fig 3 (c) the oscillation period raised from the supercritial Hopf bifurcation approaches infinity. Due to the occurrence of BT bifurcation, the infinity period oscillation may due to the homoclinic cycle bifurcating from the local BT bifurcation. Therefore, large period viral load oscillation may happen around $r = 3$ for $a = 3.8$. The large oscillation indicate HIV viral blips. The simulated viral blips are shown in Fig. 3.

Biologically, for infected T-cell population, if the proliferation (r) and death (a) are small, the healthy T-cell load can stabilize or oscillate around a high level. The infection progress with the increase of the infected cell proliferation rate (r), since the healthy T-cell load either oscillates or stabilizes in a low level. While the increase of the infected T-cell death rate shows a prohibitive effect on the disease progression. The existence of oscillations, indicating viral blips, is of interest. An increase of the oscillating region indicates that HIV infection is unlikely to stabilize in the AIDS stage. Such oscillations can be discussed in terms of viral blips. Viral blips, when large spikes in viral load occur, can be observed in HIV patients even when the patient is on highly effective therapy and has a viral load that is unobservable. In Fig. 3 we show model outcomes with very regular oscillatory behavior ((b) and (d)), and also cases that more closely reflect the occurrence of viral blips ((a) and (c)) (Zhang et al, 2014). Our analysis and simulation show that the progression in the infected T-cell proliferation and death rates could result various stages of HIV progression, including low and high level infection, regular-oscillating level infection, and viral blips.

5.2 a vs β

The influence of the infection rate β has direct implications on HIV drug therapy. We therefore provide an in-depth bifurcation analysis considering this parameter. Fig. 4 (a) shows the influence of parameters a and β on disease progression. The disease can be completely eliminated if parameters locate on the right of the saddle-node bifurcation/limit point (LP) curve in green. There is a possiblility that model (1)

(a)

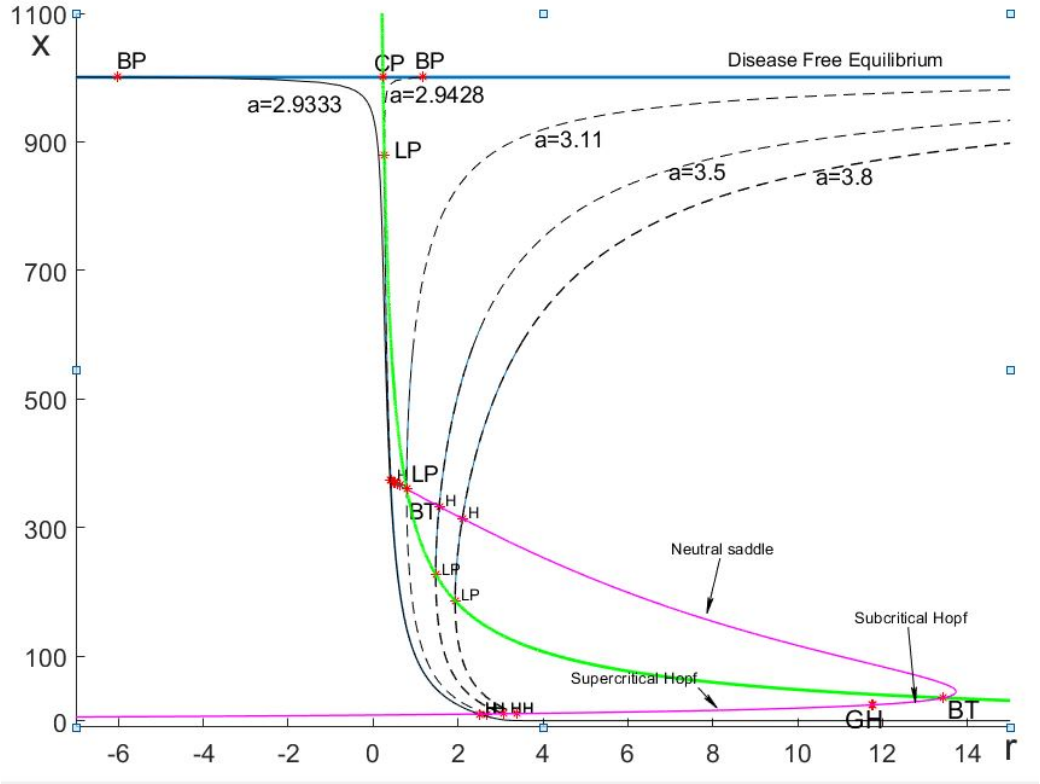

(b)

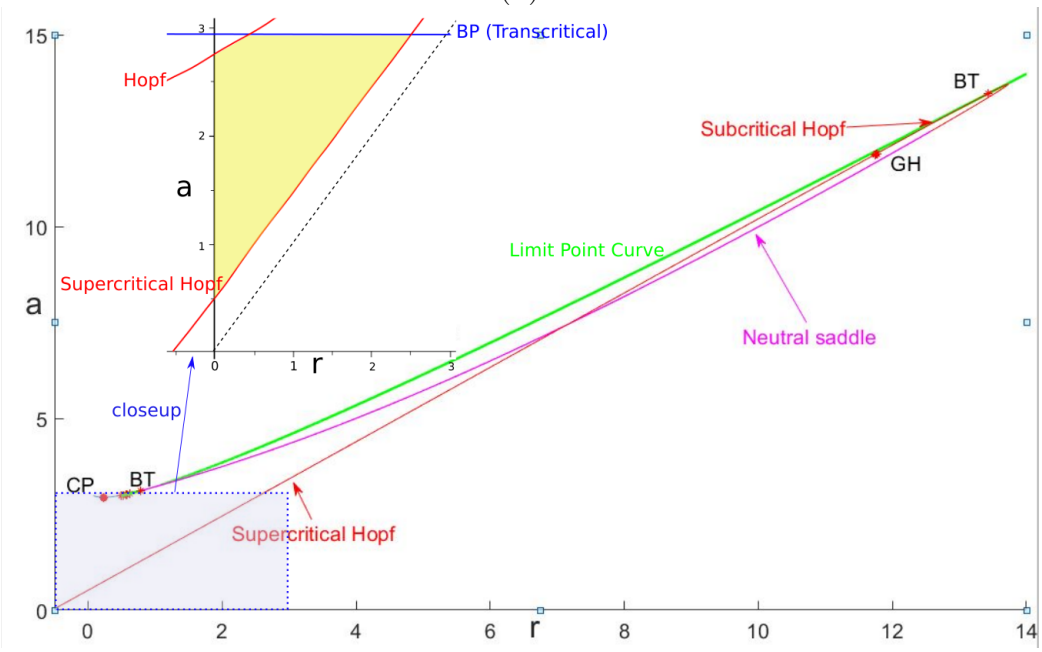

Figure 2: (a) 1-dimensional bifurcation diagram: r vs x for model (1). (b): 2-dimensional bifurcation diagram: r vs a for model (1).

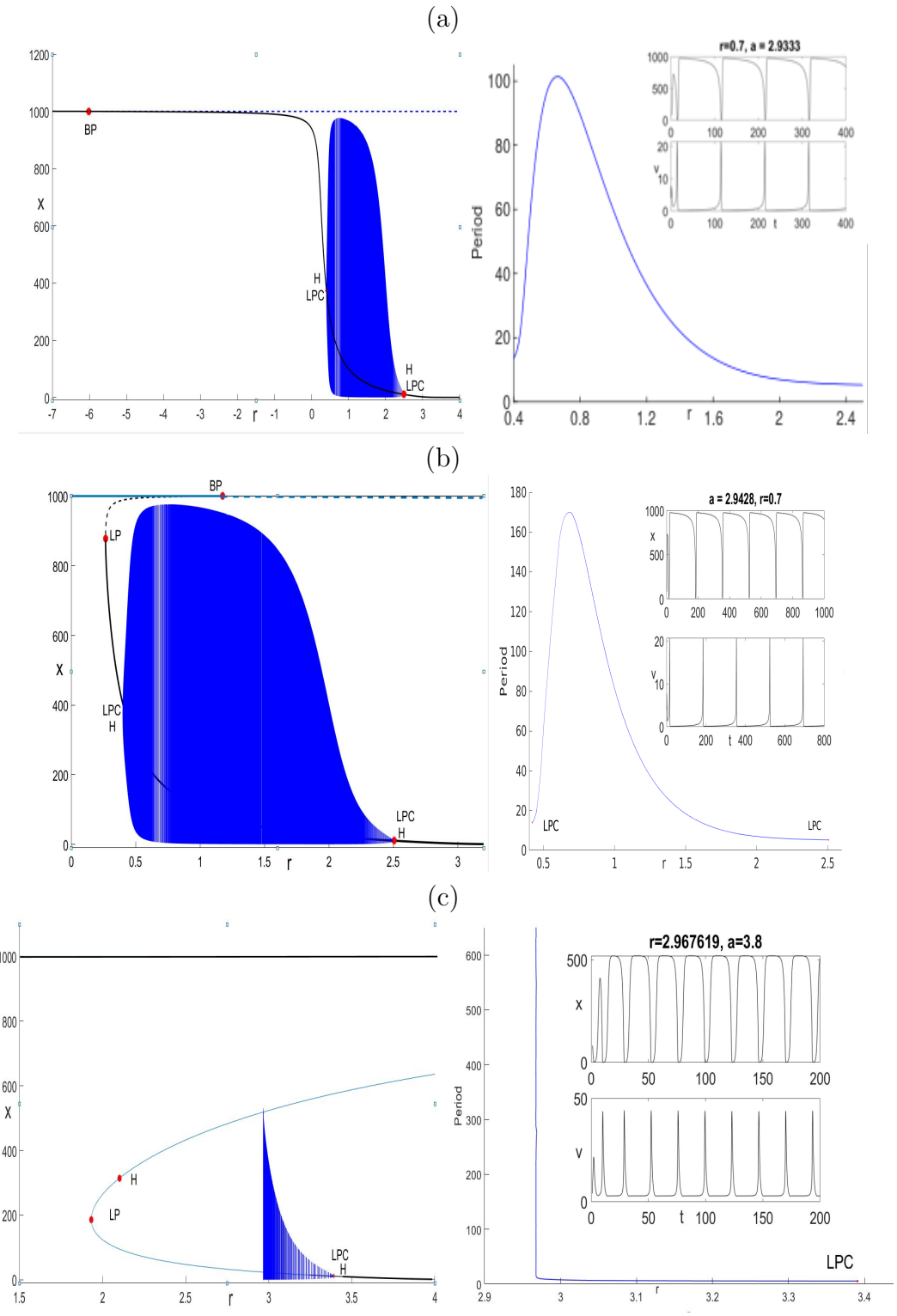

Figure 3: 1-dimensional bifurcation diagrams with $a = 2.9333, 2.9428, 3.8$ day^{-1} are plotted in the left column of (a), (b), and (c). The corresponding period vs bifurcation parameter r are plotted in the right column. Simulated viral blips are shown as inserts.

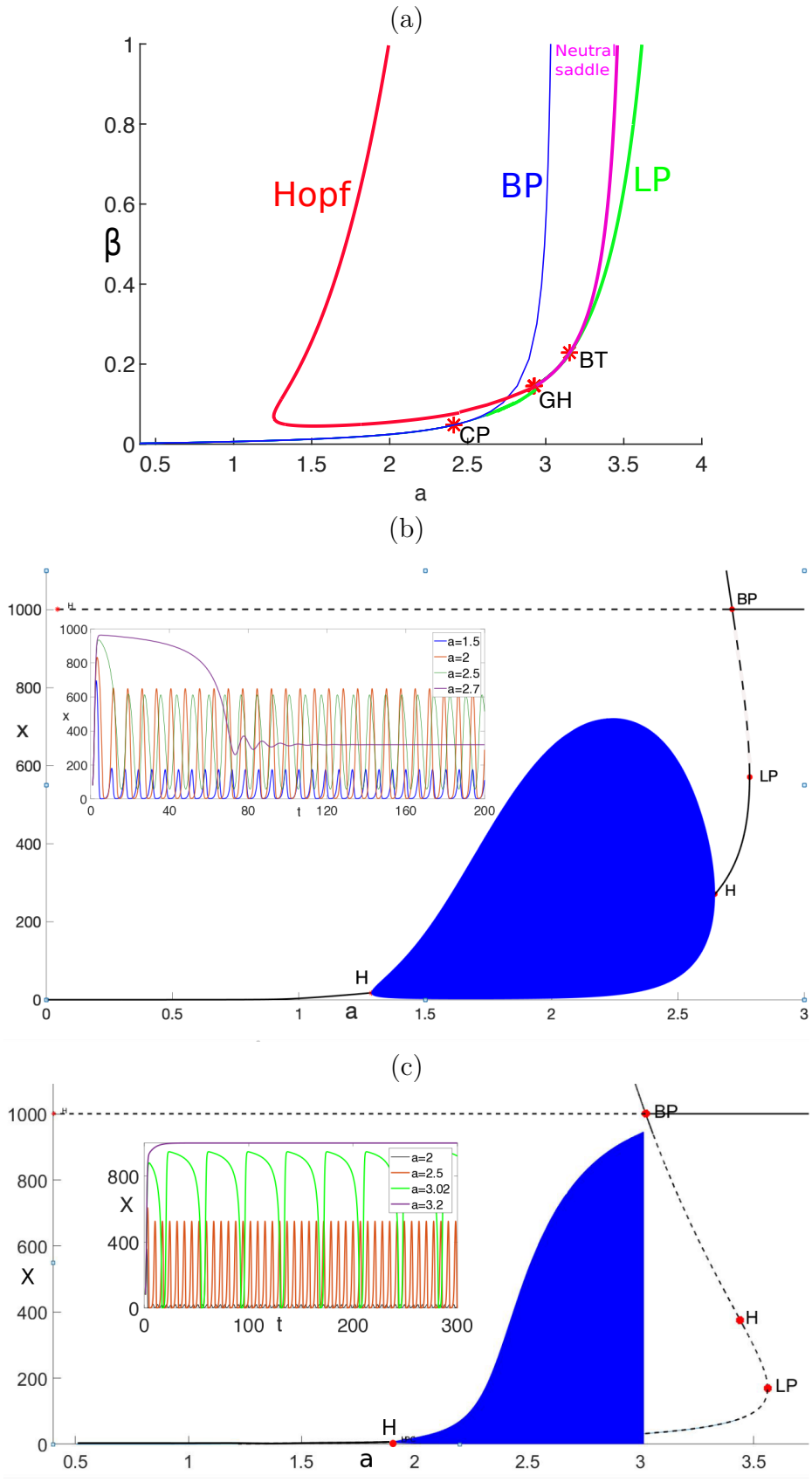

Figure 4: (a) 2-dimensional bifurcation diagram: a vs β for model (1).

shows bistable behavior in the region bounded by the green LP curve and the blue transcritical bifurcation/branching point (BP) curve. Hopf curve is plotted in red and connected with a magenta curve denoting neutral saddle at a BT bifurcation point. In the red Hopf curve, the part between BT and GH (generalized Hopf) denotes subcritical Hopf bifurcation, the rest of the curve denotes supercritical Hopf bifurcation. Oscillation occurs between two Hopf curves next to each other or between Hopf and BP curves. These two oscillation cases are further investigated. The corresponding 1-dimensional bifurcation diagrams are plotted in Fig. 4 (b) and (c) with $\beta = 0.1$ and $\beta = 0.8$, respectively..

5.3 More 2-dimensional Bifurcation Diagrams

Setting $q = 1$ and using β, a, kq, u and r as bifurcation parameters: we plot eight two-dimensional bifurcation diagrams Figure 5 (1): a vs kq, (2): r vs β, (3): r vs kq, (4): r vs u, (5): u vs a, (6): u vs kq, (7): u vs β, and (8): kq vs β. The parameter values of r, β, a, u and kq ($q = 1$) are taken from Table 2, the other parameter values are from Table 3. The positive equilibrium solution E_1 are ruled by equations (3), (7) and (34). The blue, red, magenta, and green curves denote BP, Hopf, neutral saddle, and LP bifurcation curves. The disease can be eliminated if parameters taken below the green LP curves in (1), (3) and (6), above in (5), and on the left in (8). Oscillations shown when bifurcation parameters are taken between the blue and red curves in (1), (3), (4) and (5), and within the red curves in (2), (5), (6), (7) and (8).

Since periodic solutions are of interest, both mathematically and biologically (as they are indicative of viral blips), we chose values of r and a such that $r < a$, when constant values of r and a were needed i.e., in the u vs kq, u vs β and kq vs β parameter planes. Again, the red lines denote the Hopf bifurcation curves, the blue lines show the transcritical bifurcation curves, the green curves are saddle node bifurcation curves. The regions generating periodic solutions are highlighted. These figures along with Figures 2 and 4 allow us to look at the effects of different drug therapy and immunological interventions used to fight HIV infection in patients, with the end goal of HIV virus eradication. In all cases we see that decreases in the infection rate β and the virus production rate kq are needed to achieve this goal, because the system comes to a region where the DFE is stable. These results reflect the effects of current drug therapies, which inhibit the infection of cells (reverse transcriptase inhibitors) and the production of infectious virus particles (protease inhibitors), that are used in HIV drug therapy regimens. Figures 2, 4, and 5 also show that increases in the infected cell death rate a and the virus clearance rate u, both indicators of increased immune system function, are needed to aid HIV patients. However, we also see that as β and kq decrease, and a and u increase the infected equilibrium moves to a region where oscillatory solutions can occur (when $r < a$). We also note that such large changes in β, kq, a and u may not be feasible.

Finally, we focus our attention on the proliferation/activation rate r and the bifurcation diagrams: r vs a in Figure 2 (a), r vs β in Figure 5 (2), r vs kq in

Figure 5 (3) and r vs u in Figure 5 (4) . Here, we see that to eradicate HIV within a patient, given small changes in a, kq and β, extremely large changes in r are needed (the slope of the blue line is very shallow). We also see, however, that as u increases, increases in r are also needed to achieve this goal. This means that, to eradicate HIV from a patient, the immune system must be primed to neutralize all virus particles that are produced from newly activated latently infected cells. However, increases in r will also affect the healthy CD4 T-cell count x since the proliferation rate of such cells depends on the size of the infected cell population (which represents a T-cell capacity per volume of plasma, and also immune system exhaustion if there are a large numbers of infected cells)). Therefore, we conclude that the activation of latently infected cells should only be considered in treatments if the immune system is primed to eradicate virus very quickly and effectively - a high virus clearance rate u must be achieved first.

6 Discussion

Mathematical models describing HIV infection in-host offer a way to understand the dynamics of HIV during different disease stages. The vast majority of mathematical studies in the literature focus on the acute and latent stages of infection, ignoring the progression from HIV to AIDS. We have developed a mathematical model which includes biological mechanisms that have been associated with HIV progression to AIDS. These include: thymic involution, a reduction in T-cell production by age of an individual, density dependent logistic growth in the CD4 T-cell population, and the effects of the latently infected cell pool, immune system exhaustion, and contributions of production of free virus from other cells pools.

It is currently unknown how much each of the processes listed above contribute to the health status of the host in the progression of HIV to AIDS. In the absence of the prior data on the problem that we are considering, we determine the most significant parameters which can substantially change the model output behaviors through a global uncertainty and sensitivity analysis. Statistical based Latin hypercube sampling (LHS) and partial rank correlation coefficient (PRCC) are carried out for all model parameters on clinically feasible intervals. This uncertainty and sensitivity analysis narrows down the parameters which give the most influence on the model dynamics. Bifurcation analyses are used to further examine and compare the influence that the identified parameters applied on model output. Our results point out the parameter regions for HIV progression stages: clearance, relapse, remission, and recurrence. Our numerical and analytical results not only can be related to specific biological processes, but also give the relative importance of each process. Our results reflect contributions to the productively infected CD4 T-cell pool via activation of latently infected T-cells and proliferation of productively infected CD4 T-cells (r), production of free virus from other cell pools and/or a change in production by productively infected CD4 T-cells (kq), and immune system exhaustion (a and u).

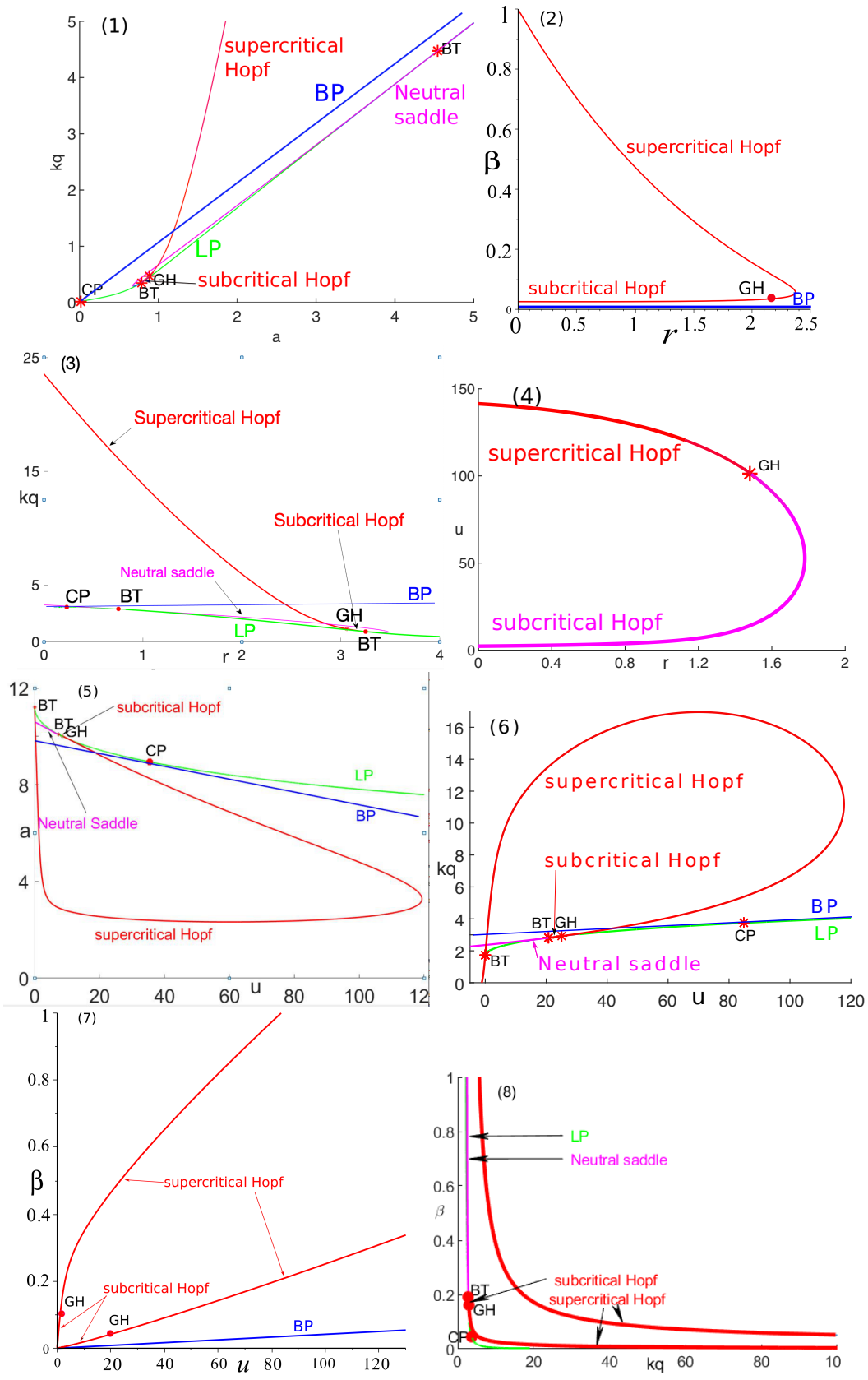

Figure 5: 2-dimensional bifurcation diagrams for the model (1).

Monocytes and dendritic cells have been implicated as HIV reservoirs using in vitro and ex vivo models of viral infection (Coleman and Wu, 2009). Monocytes and macrophages, after infection with HIV virus are resistant to cytopathic effects and persist throughout the course of infection as long-term stable reservoirs for HIV-1 which produce virus, and can disseminate the virus to tissues (Kedzierska and Crowe, 2002). Monocytes and macrophages have also been shown to contribute to the pathogenesis of HIV via the impairment of effector functions (Kedzierska and Crowe, 2002). Although it is known that HIV interacts with monocytes, macrophages and dendritic cells, some key questions remain to be answered to fully understand the pathogenesis of HIV to AIDS, including the development, persistence and activation of the latently infected cell pool. For instance, the relative contributions of these cell types in the development and persistence of the HIV latently infected cells reservoir, the activation of these cells, and the individual contributions of these cells in both viral and host aspects in the progression to AIDS remain to be elucidated. Mathematical models explicitly including these cells lines can contribute to this area of study. Our results confirm the importance of this mechanism in the HIV progression.

7 Appendix

Assumption	Reference
$x_0 \in [600, 1400]$	Shete et al (2010)
$R_0 \in [1, 40]$	Ribeiro et al (2010)
$a > r(1 - \frac{x_0}{T})$	Determined by Equation (12)
$x + y \in [200, 1400]$	200 CD4 T-cells/μL denotes AIDS diagnosis. Upper bound is the same as the range for x_0, for simplicity.

Table 1: Filter criteria for sensitivity and uncertainty analysis.

	Fig2(a)	Fig4(a)	Fig5(1)	Fig5(2)	Fig5(3)	Fig5(4)	Fig5(5)	Fig5(6)	Fig5(7)	Fig5(8)
Para.	r vs a	a vs β	a vs k	r vs β	r vs k	u vs r	u vs a	u vs k	u vs β	k vs β
r	–	1.065	1.065	–	–	–	1.22	1.22	1.22	1.22
β	0.3	–	0.3	–	0.3	0.3	0.3	0.3	–	–
a	–	–	–	2.92	2.92	2.92	–	2.943	2.943	2.943
u	13.14	13.14	13.14	13.14	13.14	–	–	–	–	13.14
kq	3.07	3.07	–	10	–	10	10	–	10	–

Table 2: Baseline parameter values:$\lambda = 96.8$, $\epsilon = 7.7$, $p = 2.6$, $T = 1001.9$ and $d = 0.016$.

8 Acknowledgements

Wenjing Zhang acknowledges start-up funding from Texas Tech University. Neal Madras is supported in part by a Discovery Grant from NSERC of Canada. Jane Heffernan is supported by a Discovery Grant and Discovery Accelerator Supplement from NSERC of Canada, and a York University Research Chair. The authors would like to thank Gillian E Wu (York University) and Jonathan Forde (Hobart and William Smith Colleges for their useful comments and suggestions.

References

Alizon S, Magnus C (2012) Modelling the course of an HIV infection: Insights from ecology and evolution. Viruses 4(10):1984–2013

Anderson RM, May RM (1992) Infectious diseases of humans: dynamics and control. Oxford University Press

Anderson TW (1958) An introduction to multivariate statistical analysis. Wiley, New York

Arnaout RA, Wodarz D, et al (2000) HIV–1 dynamics revisited: biphasic decay by cytotoxic T lymphocyte killing? Proceedings of the Royal Society of London B: Biological Sciences 267(1450):1347–1354

Beltz L (1999) Thymic involution and HIV progression. Immunology Today 20(9):429

Biesinger T, Kimata JT (2008) HIV-1 transmission, replication fitness and disease progression. Virology: research and treatment 1:VRT–S860

Bocharov G, Romanyukha A (1994) Mathematical model of antiviral immune response III. Influenza A virus infection. Journal of Theoretical Biology 167(4):323 – 360

Para.	Definition	Unit	Range	Reference
λ	Generating rate of naive T cells from thymus	$\text{day}^{-1}\mu l^{-1}$	$70 - 120$	estimated
ϵ	Viral load when T cell load decreases to half of its normal value	μl^{-1}	$10^{-5} - 10$	Perelson et al (1993)
p	Homeostatic proliferation rate of T cells	μl^{-1} cell^{-1} day^{-1}	$0.03 - 4$	Perelson et al (1993) Wang et al (2009) Wang et al (2013)
r	Infected T cells proliferation rate	$\mu l^{-1}\text{cell}^{-1}$ day^{-1}	$10^{-5} - 3$	Wang et al (2013)
T	Maximum T cell population level	μl^{-1}	$800 - 1200$	Perelson et al (1993) Heffernan and Wahl (2006b) Wang et al (2013)
β	Infection rate of healthy T cell by HIV virus infected	μl^{-1} cell^{-1} virus^{-1} day^{-1}	$10^{-5} - 0.5$	Culshaw et al (2004) Wang et al (2009) Wang et al (2013)
d	Death rate of uninfected T cells	μl^{-1} cell^{-1} day^{-1}	$0.007 - 0.1$	Arnaout et al (2000) Culshaw et al (2004) Perelson et al (1993)
a	Death rate of infected T cells	μl^{-1} cell^{-1} day^{-1}	$0.5 - 1.4$	Markowitz et al (2003) Perelson et al (1996)
u	Clearance rate	μl^{-1} virus^{-1} day^{-1}	$3 - 36$	Perelson et al (1996) Ramratnam et al (1999)
kq	Number of virus produced by lysing an infected T cell	μl^{-1} cell^{-1} day^{-1}	$6 - 3000$	Smith and De Leenheer (2003) Rong et al (2007) Rong and Perelson (2009)

Table 3: List of parameter values of model (1)

Callaway DS, Perelson AS (2002) HIV-1 infection and low steady state viral loads. Bulletin of mathematical biology 64(1):29–64

Castillo-Chavez C, Song B (2004) Dynamical models of tuberculosis and their applications. Mathematical biosciences and engineering 1(2):361–404

Chomarat P, Dantin C, Bennett L, Banchereau J, Palucka AK (2003) TNF skews monocyte differentiation from macrophages to dendritic cells. The Journal of Immunology 171(5):2262–2269

Chomont N, El-Far M, Ancuta P, Trautmann L, Procopio FA, Yassine-Diab B, Boucher G, Boulassel MR, Ghattas G, Brenchley JM, et al (2009) Hiv reservoir size and persistence are driven by T cell survival and homeostatic proliferation. Nature medicine 15(8):893

Chun TW, Engel D, Berrey MM, Shea T, Corey L, Fauci AS (1998) Early establishment of a pool of latently infected, resting CD4+ T cells during primary HIV-1 infection. Proceedings of the National Academy of Sciences 95(15):8869–8873

Cloyd MW, Chen JJ, Wang L (2000) How does HIV cause AIDS? the homing theory. Molecular Medicine Today 6(3):108–111

Coleman CM, Wu L (2009) HIV interactions with monocytes and dendritic cells: viral latency and reservoirs. Retrovirology 6(1):51

Culshaw RV (2006) Mathematical modeling of AIDS progression: limitations, expectations, and future directions. Journal of American Physicians and Surgeons 11(4):101

Culshaw RV, Ruan S, Spiteri RJ (2004) Optimal HIV treatment by maximising immune response. Journal of Mathematical Biology 48(5):545–562

Cunningham AL, Donaghy H, Harman AN, Kim M, Turville SG (2010) Manipulation of dendritic cell function by viruses. Current Opinion in Microbiology 13(4):524 – 529, host-Microbe Interactions: Fungi/Parasites/Viruses

Dahabieh MS, Battivelli E, Verdin E (2015) Understanding HIV latency: the road to an HIV cure. Annual review of medicine 66:407–421

Van den Driessche P, Watmough J (2002) Reproduction numbers and sub-threshold endemic equilibria for compartmental models of disease transmission. Mathematical biosciences 180(1-2):29–48

Dubrow R, Silverberg MJ, Park LS, Crothers K, Justice AC (2012) HIV infection, aging, and immune function: implications for cancer risk and prevention. Current opinion in oncology 24(5):506

Feinberg MB, McLean AR (1997) AIDS: Decline and fall of immune surveillance? Current Biology 7(3):R136 – R140

Fraser C, Lythgoe K, Leventhal GE, Shirreff G, Hollingsworth TD, Alizon S, Bonhoeffer S (2014) Virulence and pathogenesis of HIV-1 infection: an evolutionary perspective. Science 343(6177):1243,727

G Meissner E, M Duus K, Loomis R, DAgostin R, Su L (2003) HIV-1 replication and pathogenesis in the human thymus. Current HIV research 1(3):275–285

Ginhoux F, Jung S (2014) Monocytes and macrophages: developmental pathways and tissue homeostasis. Nature Reviews Immunology 14(6):392–404

Grossman Z, Feinberg MB, Paul WE (1998) Multiple modes of cellular activation and virus transmission in HIV infection: a role for chronically and latently infected cells in sustaining viral replication. Proceedings of the National Academy of Sciences 95(11):6314–6319

Hancioglu B, Swigon D, Clermont G (2007) A dynamical model of human immune response to influenza A virus infection. Journal of Theoretical Biology 246(1):70 – 86

Hazenberg MD, Otto SA, van Benthem BH, Roos MT, Coutinho RA, Lange JM, Hamann D, Prins M, Miedema F (2003) Persistent immune activation in HIV-1 infection is associated with progression to AIDS. Aids 17(13):1881–1888

Heffernan J, Keeling M (2008) An in-host model of acute infection: Measles as a case study. Theoretical Population Biology 73(1):134 – 147, DOI https://doi.org/10.1016/j.tpb.2007.10.003

Heffernan J, Wahl L (2006a) Improving estimates of the basic reproductive ratio: Using both the mean and the dispersal of transition times. Theoretical Population Biology 70(2):135 – 145

Heffernan JM, Wahl LM (2006b) Natural variation in HIV infection: Monte Carlo estimates that include cd8 effector cells. Journal of Theoretical Biology 243(2):191 – 204

Hsu DC, Sereti I (2014) Chronic immune activation in HIV. Encyclopedia of AIDS pp 1–10

Kedzierska K, Crowe SM (2002) The role of monocytes and macrophages in the pathogenesis of HIV-1 infection. Current medicinal chemistry 9(21):1893–1903

Klasse P (2015) Molecular determinants of the ratio of inert to infectious virus particles. In: Progress in molecular biology and translational science, vol 129, Elsevier, pp 285–326

Klatt NR, Chomont N, Douek DC, Deeks SG (2013) Immune activation and HIV persistence: implications for curative approaches to HIV infection. Immunological reviews 254(1):326–342

Koppensteiner H, Brack-Werner R, Schindler M (2012) Macrophages and their relevance in human immunodeficiency virus type I infection. Retrovirology 9(1):82

Kwa D, Vingerhoed J, Boeser-Nunnink B, Broersen S, Schuitemaker H (2001) Cytopathic effects of non-syncytium-inducing and syncytium-inducing human immunodeficiency virus type 1 variants on different CD4+-T-cell subsets are determined only by coreceptor expression. Journal of virology 75(21):10,455–10,459

Langford SE, Ananworanich J, Cooper DA (2007) Predictors of disease progression in HIV infection: a review. AIDS research and therapy 4(1):11

Marden M (1989) Geometry of Polynomials. American Mathematical Society, Providence

Marino S, Hogue IB, Ray CJ, Kirschner DE (2008) A methodology for performing global uncertainty and sensitivity analysis in systems biology. Journal of theoretical biology 254(1):178–196

Markowitz M, Louie M, Hurley A, Sun E, Di Mascio M, Perelson AS, Ho DD (2003) A novel antiviral intervention results in more accurate assessment of human immunodeficiency virus type 1 replication dynamics and T-cell decay in vivo. Journal of virology 77(8):5037–5038

McKay MD, Beckman RJ, Conover WJ (1979) Comparison of three methods for selecting values of input variables in the analysis of output from a computer code. Technometrics 21(2):239–245

Murray J, et al (1989) Mathematical Biology. Mathematical Biology (19)

Nowak M, May RM (2000) Virus dynamics: mathematical principles of immunology and virology: mathematical principles of immunology and virology. Oxford University Press, UK

Orenstein JM, Fox C, Wahl SM (1997) Macrophages as a source of HIV during opportunistic infections. Science 276(5320):1857–1861

Paiardini M, Müller-Trutwin M (2013) HIV-associated chronic immune activation. Immunological reviews 254(1):78–101

Perelson AS, Kirschner DE, De Boer R (1993) Dynamics of hiv infection of CD4+ T cells. Mathematical biosciences 114(1):81–125

Perelson AS, Neumann AU, Markowitz M, Leonard JM, Ho DD (1996) HIV-1 dynamics in vivo: virion clearance rate, infected cell life-span, and viral generation time. Science 271(5255):1582–1586

Ramratnam B, Bonhoeffer S, Binley J, Hurley A, Zhang L, Mittler JE, Markowitz M, Moore JP, Perelson AS, Ho DD (1999) Rapid production and clearance of HIV-1 and hepatitis C virus assessed by large volume plasma apheresis. The Lancet 354(9192):1782–1785

Ribeiro RM, Qin L, Chavez LL, Li D, Self SG, Perelson AS (2010) Estimation of the initial viral growth rate and basic reproductive number during acute HIV-1 infection. Journal of virology 84(12):6096–6102

Rong L, Perelson AS (2009) Modeling latently infected cell activation: viral and latent reservoir persistence, and viral blips in HIV-infected patients on potent therapy. PLoS computational biology 5(10):e1000,533

Rong L, Feng Z, Perelson AS (2007) Emergence of HIV-1 drug resistance during antiretroviral treatment. Bulletin of mathematical biology 69(6):2027–2060

Ruelas DS, Greene WC (2013) An integrated overview of HIV-1 latency. Cell 155(3):519–529

Selhorst P, Combrinck C, Ndabambi N, Ismail SD, Abrahams MR, Lacerda M, Samsunder N, Garrett N, Karim QA, Karim SSA, et al (2017) Replication capacity of viruses from acute infection drives HIV-1 disease progression. Journal of virology 91(8):e01,806–16

Sereti I, Altfeld M (2016) Immune activation and HIV: an enduring relationship. Current Opinion in HIV and AIDS 11(2):129

Shete A, Thakar M, Abraham PR, Paranjape R (2010) A review on peripheral blood CD4+ T lymphocyte counts in healthy adult indians. The Indian journal of medical research 132(6):667

Smith HL, De Leenheer P (2003) Virus dynamics: A global analysis. SIAM Journal on Applied Mathematics 63(4):1313–1327

Surh CD, Sprent J (2000) Homeostatic T cell proliferation: how far can T cells be activated to self-ligands? Journal of Experimental Medicine 192(4):F9–F14

Thieme HR (2003) Mathematics in population biology. Princeton University Press

Till MA, Ghetie V, Gregory T, Patzer EJ, Porter JP, Uhr JW, Capon DJ, Vitetta ES (1988) HIV-infected cells are killed by rCD4-ricin A chain. Science 242(4882):1166–1168

Van Lint C, Bouchat S, Marcello A (2013) HIV-1 transcription and latency: an update. Retrovirology 10(1):67

Vazeux R, Brousse N, Jarry A, Henin D, Marche C, Vedrenne C, Mikol J, Wolff M, Michon C, Rozenbaum W, et al (1987) AIDS subacute encephalitis: identification of HIV-infected cells. The American journal of pathology 126(3):403

Wang Y, Zhou Y, Wu J, Heffernan J (2009) Oscillatory viral dynamics in a delayed HIV pathogenesis model. Mathematical Biosciences 219(2):104–112

Wang Y, Zhou Y, Brauer F, Heffernan JM (2013) Viral dynamics model with CTL immune response incorporating antiretroviral therapy. Journal of mathematical biology 67(4):901–934

Wodarz D, Nowak MA (2002) Mathematical models of HIV pathogenesis and treatment. BioEssays 24(12):1178–1187

Ye P, Kirschner DE, Kourtis AP (2004) The thymus during HIV disease: role in pathogenesis and in immune recovery. Current HIV research 2(2):177–183

Zhang W, Wahl LM, Yu P (2014) Viral blips may not need a trigger: how transient viremia can arise in deterministic in-host models. SIAM Review 56(1):127–155

Zhang W, Wahl LM, Yu P (2016) Backward bifurcations, turning points and rich dynamics in simple disease models. Journal of Mathematical Biology pp 1–30